Damage Tolerance of Fully Orthotropic Laminates in Compression

Neil Baker and Richard Butler
Department of Mechanical Engineering, University of Bath, Bath, UK
Christopher B. York
Aerospace Sciences, School of Engineering, University of Glasgow, Glasgow, UK

1 Abstract

The compression after impact (CAI) strength of fully orthotropic composite laminates with up to 21 plies is presented, as analysed by an existing strip model. Candidate layups, which can be symmetric, anti-symmetric or non-symmetric, are preselected to exhibit no elastic coupling response, with manufacturing rules applied. These criteria, along with the use of a simple surrogate sublaminate buckling model, were chosen to allow analysis of all feasible laminates in the design space without excessive computation time. Results indicate that although the inclusion of non-symmetric layups in the design space does not give benefits with respect to maximum achievable damage tolerance, these laminates can exhibit damage tolerance close to that of an anti-symmetric design for some ply counts, and better than symmetric solutions in most cases. It is also noted that in some instances increasing the number of plies in a laminate can actually reduce the highest achievable threshold load for damage tolerance, as a result of the large influence Poisson's ratio has on sublaminate buckling. Average errors in the surrogate model were low in all cases, with maximum non-conservative errors less than 1%. The surrogate buckling model reduced computational time by over 99% when compared to the fully exhaustive search.

2 Keywords

A. Laminate, Polymer Matrix Composites. C. Damage Tolerance. Non-Symmetric.

3 Nomenclature

A_{11} = axial stiffness of delaminated sublaminate

E_{11} = longitudinal elastic modulus

E_{22} = transverse elastic modulus

G_{12} = shear modulus

G = strain energy release rate

G_{IC} = critical Mode I fracture energy of resin

l = delamination length

N = total number of plies in laminate

T = laminate thickness

t = ply thickness

U_1 = sublaminate bending energy

U_2 = sublaminate membrane energy

ε^C = critical buckling strain

ε_{th} = threshold propagation strain

ν_{12} = major Poisson's ratio

ν_{xy} = laminate Poisson's ratio

σ_{th} = threshold propagation stress

4 Introduction

Propagation of delamination damage in composites under uniaxial compression is often driven by opening mode buckling of thin film sublaminates. The load at which this propagation occurs is dependent on the full laminate layup, but is especially sensitive to the layup of the thin surface sublaminates produced by delaminations. As barely visible impact damage (BVID) is almost always non-symmetric through the thickness, symmetric laminates may not be the optimum configuration with regard to damage tolerance in applications where

the impact threat is not equal for the two faces of the laminate. This condition is true in most composite applications, but especially pronounced in areas such as the skins of composite sandwich panels (Fig. 1(a)), which can only be subject to impact on their outer face. In this case, usage of symmetric laminates means that one face of the laminate may be unnecessarily damage tolerant, and the stipulation of a symmetric layup not only restricts the number of designs available to a designer, but may also actively discount those layups that are best suited to the application. Other instances might include the flanges of stiffeners, where non-symmetry may arise from manufacturing requirements (Fig. 1(b)). Current design practice generally dictates however that laminates should be symmetric to ensure that there is no in-plane/out-of-plane coupling, although these designs usually display bend-twist coupling. In this work, complete listings of fully orthotropic laminates up to 21 plies thick are analysed using an existing compression after impact (CAI) strip model to assess the benefits of non-symmetry with regards to damage tolerance.

Previous work presented by the authors looked at the use of optimisation techniques to maximize the damage tolerance of composite laminates, but it was found that even the most general of optimisation techniques was difficult to tune to converge reliably. The focus of this work will instead be to draw attention to the potential of applying design constraints to downsize the selectable design space, before using simple surrogate modelling to remove much of the computational burden when analysing those designs for damage tolerance. Such methodology presents the possibility of analysing the entire potential design space quickly and efficiently for thinner sublaminates, without the worries of converging to local optima.

5 Compression after Impact Modelling

5.1 Strip Model

An approximate, closed form CAI model, previously presented[1], is used in this work to estimate CAI strength of a design space of fully orthotropic laminates. The model assumes

that delamination growth is initiated in either the loading direction or in the transverse direction, and that it is driven by local buckling of a thin delaminated region, henceforth referred to as the sublaminate. It is also assumed that the base substrate remains flat before sublaminate buckling, and in the locally post-buckled regime and at propagation (see Fig. 2). Strain energy released as a result of delamination growth in the longitudinal or transverse direction is assumed to produce Mode I fracture of the resin material. In reality, the propagation is more complex than is assumed, since growth is mixed mode and may initiate in the transverse direction, particularly when there is interaction between buckling of the thin sublaminate and that of the laminate. However, the method has been shown to produce accurate lower bound predictions of threshold strain for a range of experimental test laminates[2]. Hence it is used here as a very efficient method for predicting the CAI strength of composite laminates. In the following, the model is described for propagation in the direction of applied strain before considering the case of transverse propagation.

The CAI model[1] compares the energy within the thin sublaminate before and after a propagation event has occurred, and equates this to the critical Mode I strain energy release rate (SERR) for the resin. Energy is defined in terms of applied strain ε, sublaminate buckling strain ε^C and laminate axial stiffness A_{11}. Buckling of the sublaminate is analysed using the infinite strip buckling program VICONOPT[3], with sublaminate loads calculated from classical laminated plate theory, assuming strain compatibility at the boundary between the flat, uniaxially-loaded laminate and the delaminated region. It is assumed that load is applied as end shortening, along the sublaminate neutral plane; hence loading is purely in-plane. As a result of strain compatibility at the delamination boundary, transverse and shear loads may be induced in the sublaminate due to, respectively, mismatches between the Poisson's ratio of the full laminate and the sublaminate, and sublaminate extension-shear coupling. Delaminations are modelled as circular, using six equal width strips. The influence of

boundary conditions and the number of nodes used in the VICONOPT buckling model have previously been explored[4]. Bending energy stored in the buckled sublaminate is equated to the applied in-plane energy[5], leading to Eq. (1) for bending energy.

$$U_1(l) = A_{11} l(\varepsilon - \varepsilon^C)\varepsilon^C \tag{1}$$

Similarly, membrane energy can be approximated as:

$$U_2(l) = \frac{A_{11}}{2} l(\varepsilon^C)^2 \tag{2}$$

Finally, membrane energy is also released from the region into which the delamination propagates. If propagation extends the delamination by δl in Fig. 2(b), then this energy is described as in Eq. (3).

$$U_2^* = \frac{A_{11}}{2} \int_0^{\delta l} \varepsilon^2 dx \tag{3}$$

The bending and membrane energy can be calculated immediately after a propagation of δl by replacing l with $l + \delta l$ in Eqs. (1) and (2). Equations (1-3) can then be combined to determine the energy available for propagation at a given applied strain, as shown in Eq. (4).

$$G = \lim_{\delta l \to 0} \left\{ U_1(l) - U_1(l+\delta l) + U_2(l) - U_2(l+\delta l) + U_2^* \right\} \frac{1}{\delta l} \tag{4}$$

Hence

$$G = \frac{A_{11}}{2} (\varepsilon - \varepsilon^C)(\varepsilon + 3\varepsilon^C) \tag{5}$$

Note that this is the expression derived by Chai et al.[6] for one-dimensional propagation, except that here it covers a composite sublaminate of axial stiffness A_{11} and two-dimensional sublaminate buckling. In this case it is assumed the sublaminate has no post-buckled stiffness. This assumption gives a lower bound solution, and is more fully discussed elsewhere[4]. Equation (5) is then rearranged in terms of applied strain ε. By setting G to the critical Mode I SERR of the resin material G_{IC}, the threshold propagation strain ε_{th} may be

approximated. This yields Eq. (6), describing threshold propagation strain of interface i ($\varepsilon_{th,i}$) in terms of local buckling strain ε_i^C, the axial stiffness of the buckled sublaminate $A_{11,i}$, and the critical Mode I SERR of the resin material G_{IC}. This equation is applied at each delamination individually, assuming an otherwise undamaged laminate. In this work Eq. (6) is applied at each individual ply interface up to a quarter of the laminate thickness, i.e. to $n=N/4$.

$$\varepsilon_{th,i} = -\varepsilon_i^C \left(1 - \sqrt{4 + \frac{2G_{IC}}{A_{11,i}\left(\varepsilon_i^C\right)^2}} \right) \quad , \quad i = 1, 2, \ldots n \tag{6}$$

Validation of this model for a range of sublaminate types has previously been performed[7]. It has also been shown that the model can be adapted to predict transverse propagation through a formulation of equivalent Mode-I energy[8]. This results in a similar expression to Eq. (6), but with sublaminate axial stiffness $A_{11,i}$ replaced with sublaminate transverse stiffness $A_{22,i}$. Both expressions are employed here, the lowest value of $\varepsilon_{th,i}$ gives the prediction of threshold propagation strain.

The benefit of such a model is largely the speed with which analysis can be performed. Due to the buckling analysis of n unconnected sublaminates the model is well suited to parallelization, and as a result a single 32 ply laminate can be analysed in under one second. Even so, for larger design spaces this may not be fast enough, so a simple surrogate model of sublaminate buckling is presented as a method of further improving speed.

5.2 Surrogate Sublaminate Buckling Model

The most computationally expensive part of the CAI model is the buckling analysis applied to each of the thin film sublaminates caused as a result of delamination damage. In calculating the buckling strain of a single sublaminate, the VICONOPT model requires three inputs: the layup of the sublaminate, a definition of the damage morphology, and the Poisson's ratio of the full laminate. These inputs define the geometry of the problem, and the

loads in the sublaminate under full laminate uniaxial loading. Equation (7) shows the relationship between full laminate applied strain and sublaminate loads.

$$\begin{Bmatrix} N_x \\ N_y \\ N_{xy} \end{Bmatrix}_{sublam} = \begin{bmatrix} A_{11} & A_{12} & A_{16} \\ A_{12} & A_{22} & A_{26} \\ A_{16} & A_{26} & A_{66} \end{bmatrix}_{sublam} \begin{Bmatrix} \varepsilon \\ \varepsilon \nu_{xy} \\ 0 \end{Bmatrix} \quad (7)$$

where ε is the reference applied end shortening, and ν_{xy} is the full laminate Poisson's ratio. The CAI model approximates delamination damage as circular, so diameter is the only variable defining delamination shape. In the case of this work, delamination damage is assumed to be of constant diameter across all laminates. This is consistent with airworthiness requirements, which are based upon the detectability of impact damage, not the energy required to produce it. Hence, for a given sublaminate layup of given material, buckling strain varies only with full laminate Poisson's ratio. A simple relationship can be obtained between full laminate Poisson's ratio and buckling strain for each individual sublaminate. In the case of laminates up to 21 plies thick all sublaminate layups up to 5 plies thick need to be characterized, of which there are 1,364. Sublaminate buckling analysis within VICONOPT does not account for contact with the base substrate, so further reductions in computational requirements are made by not duplicating analysis of sublaminate layups that are mirrored about the midplane, i.e. a [45/0] sublaminate is equivalent to a [0/45] sublaminate. Similarly, layups mirrored about the 0° ply direction will also result in the same buckling strain, so for example a [45/0] sublaminate will buckle at the same full laminate end shortening as a [-45/0] sublaminate.

As can be seen in Fig. 3, the relationship between sublaminate buckling strain and full laminate Poisson's ratio is monotonic. For each sublaminate, 12 VICONOPT analyses were performed at evenly spaced values of full laminate Poisson's ratio. The number of analyses was chosen as a result of using a quad-core processor, making computation in sets of four most efficient. This buckling data was stored in a database, from which interpolation could be

performed to ascertain the buckling strain of any given sublaminate for any given value of full laminate Poisson's ratio. Due to the nature of the CAI model (see Eq. (6)), threshold strain is reasonably insensitive to errors in buckling strain predictions, so the fitting technique is not required to give excessively accurate estimations of buckling strain. Figure 4 shows the relationship between buckling strain and threshold strain for selected sublaminates in a 21 ply laminate. The quadratic relationship means that when buckling strains occur near the minimum threshold strain the model is very insensitive to errors in buckling strain, as for example in the 30mm diameter 3 ply sublaminate in Fig. 4. However, if the buckling strain lies away from the turning point errors translated from buckling strain to threshold strain become nearer 1:1. For the purposes of this work, correlation of the relationship between sublaminate buckling strain and full laminate Poisson's ratio is performed using linear interpolation between the 12 analysis points described above. Hence, the results gained give a lower bound on computation time. An initial indication of errors incurred is discussed later.

6 Characterization of Non-Symmetric Uncoupled Laminates

The Engineering Sciences Data Unit (ESDU) provides a definitive list of fully orthotropic laminates[9], derived from original work by Bartholomew[10], where fully orthotropic and fully uncoupled laminates are synonymous. Fully orthotropic laminates are those for which the extensional matrix **A** is fully orthotropic, the coupling matrix **B** is null, and the bending matrix **D** is fully orthotropic. Full orthotropy in the extensional and bending matrices is fulfilled when, respectively,

$$A_{16} = A_{26} = 0 \tag{7}$$

and

$$D_{16} = D_{26} = 0 \tag{8}$$

Fully orthotropic laminates may be desirable when compared to traditional balance symmetric layups as a result of possessing no bend-twist coupling (Eq. (8)), which may have a detrimental effect on the buckling performance of the laminate[11]. The published data[9] contains 75 symmetric sequences, for laminates with up to 21 plies, and 653 anti-symmetric sequences, for laminates with up to 20 plies, together with 49 additional non-symmetric (referred to as asymmetric) sequences, which were derived by combining symmetric and anti-symmetric sequences. The listing reveals that there are no fully uncoupled laminates, containing angle-plies, with fewer than 7 layers; the first fully uncoupled laminate is a single generic 7-ply anti-symmetric stacking sequence. This number increases to 233 generic anti-symmetric sequences with 20 plies. There are no fully uncoupled symmetric stacking sequences with less than 12 plies, and only 25 generic combinations with 20 plies. These twenty-five generic stacking sequences possess balanced and symmetric combinations of angle plies, together with cross plies, which may be 0 and/or 90°, symmetrically disposed about the laminate mid-plane; all possess angle-ply layers on the outer surfaces of the laminate. The derivation[10] adopted in the ESDU data item[9], makes the explicit assumption that cross plies, as well as angle plies, are symmetrically disposed about the laminate mid-plane, i.e. the mixing of 0 and 90° plies is permitted only in one half of the laminate, which is then reflected symmetrically about the laminate mid-plane. This rule applies to both symmetric and anti-symmetric angle-ply stacking sequences.

The relatively small number of fully orthotropic sequences for thin laminates clearly leaves limited scope for composite tailoring and was the key motivation leading to the redevelopment of a definitive list[12] for fully uncoupled laminates with up to 21 plies. In the derivation of this list for (but not restricted to) standard angle-ply configurations, i.e. ±45, 0 and 90°, the general rule of symmetry is relaxed. Cross plies, as well as angle plies, are therefore no longer constrained to be symmetric about the laminate mid-plane, leading to an

increase in the number of possible solutions. To avoid the trivial solution of a stacking sequence with cross plies only, all sequences have an angle-ply on the top outer surface of the laminate, which is in keeping with damage tolerance heuristics. As a result, the bottom outer surface may have an angle-ply of equal or opposite orientation or a cross ply, which may be either 0 or 90°. This relaxation of the rule of symmetry leads to a vastly increased design space; for 16 ply laminates, there are approximately one billion (1×10^9) possible stacking sequence combinations, of which 360 are fully uncoupled, increasing to approximately one trillion (1×10^{12}) combinations for 21 plies, with a hundred-fold increase in the number of fully uncoupled laminates. The numbers of sequences for each ply number grouping are summarized in Table 1, which reveals that symmetric laminates in fact account for a very small percentage of the design space. It should be noted that the stacking sequences derived are *fully uncoupled* with no bend-twist coupling effects. However, balanced and symmetric configurations continue to be used in studies where the effect of bend-twist coupling is simply ignored, such as those of the World-Wide Failure Exercise[13-15]. Many other studies of flexural behaviour, e.g., buckling, post-buckling, low velocity impact response, etc., continue to adopt bend-twist coupled laminates as the preferred benchmark configuration, but few consider the effects of the coupling response. For instance, it is now well understood that bend-twist coupling reduces the buckling strength of compression loaded laminated plates, but the magnitude of this strength reduction[11] is often not considered. It is therefore arguably more difficult for the composite laminate designer to apply the lessons learned in such studies when faced with different laminate designs. Laminates chosen in this study adhere strictly to the definitive listing of fully uncoupled laminates and therefore the conclusions drawn will be independent of the previously un-quantified effect of bend-twist coupling.

7 Analysis

The CAI model was applied to every fully orthotropic laminate up to 21 plies thick, as previously characterized by York[12]. Due to the thin film assumption of the model it was applied up to sublaminates 25% thick, on both faces. Note that deeper delaminations are more likely to remain closed when subject to compressive load. Delamination diameters were fixed at 30mm for all laminates. Constant delamination diameters were used through-thickness as this gives a worst-case lower bound solution in the absence of a suitable damage modelling method. Any non-symmetric laminates in the design space were analysed for damage tolerance of both faces, with the highest damage tolerance designating the damage tolerance of the laminate. This implies that the laminate would be employed in an environment where impact threats are much larger in magnitude for one face than the other, and that the laminate would be oriented as such. The properties of the material used in the analysis is detailed in Table 2[16].

As well as forcing full orthotropy in the laminate, manufacturing constraints were also applied, as detailed by Niu[17]. In particular, no more than three layers of the same angle ply were allowed consecutively within the laminate. Niu also recommends a minimum of 10% each of 0º, 90º and ±45º fibres, but this was disregarded as loading is uniaxial in this work. Manufacturing rules pertaining to damage tolerance were also ignored in the presence of the CAI modelling being performed. Results were generated using both VICONOPT sublaminate buckling analysis, and the surrogate sublaminate buckling model.

8 Results

Table 3 outlines those laminates with the best damage tolerance for each thickness, and Fig. 5 shows the threshold stress of the most damage tolerant laminates by ply percentage breakdown. Figure 6 details the best laminates at each ply count, both overall and within the available non-symmetric designs. The results in these tables and figures have been generated

using full VICONOPT analysis throughout so that they may be discussed independently of the surrogate buckling model. All laminates were also analysed using the surrogate sublaminate buckling model, Fig. 7 shows the resulting errors in threshold strain solutions, where both mean and peak error values are given.

9 Discussion

Each of the best designs shown in Table 3 exhibits traits highlighted to be beneficial to damage tolerance in previous work[1,18], namely that the outer layers are softer in the loading direction, with central layers dominated by stiffer plies. This configuration produces higher buckling strains for the thin sublaminates, and also means they accrue strain energy more slowly in the post-buckled regime. Stiffer plies in the core of the laminate increase the effective modulus, raising the threshold stress. As the model incorporates both the axial and transverse stiffnesses of the sublaminates, the best designs have similar values of sublaminate A_{11} and A_{22}. If either of these were excessively high, i.e. if the sublaminates had large numbers of 0º or 90º plies, then threshold strain would drop significantly, leading to a non-optimal solution. Figure 5 gives an indication of the best ply percentage breakdowns for damage tolerance. It can be seen that the best layups are generally those with over 40% 0º fibres, and 15% or less 90º. Within this region lie commonly used ply breakdowns in skins (44/44/12) and stiffeners (60/30/10), so these layups are practical for use in aerospace from an in-plane stiffness perspective. It should be noted however that although these laminates are similar to currently used laminates in terms of ply breakdowns, the layups are significantly different in their distribution of plies through thickness.

The general trend of peak threshold stress with respect to ply count (Fig. 6) is affected by a number of factors. Firstly, the small number of fully orthotropic candidate laminates at lower ply numbers means that no conclusions may be drawn up to 9 plies thickness. Secondly, a step change in the relationship is seen between 13 and 14 plies, the point at which an extra

ply is added to the CAI analysis within the 25% thin film sublaminate. This new sublaminate gives a lower threshold stress and so drops the damage tolerance of the 14 ply laminate. This feature is not seen for the next increase in number of sublaminates between 17 and 18 plies, as the design space is at this point large enough that a good solution may still be found. Finally, when the ply blocking manufacturing constraints becomes an issue at 14 plies, 90º fibres need to be used to unblock the central 0º plies as in many cases the addition of only a pair of ±45º plies would cause bend-twist coupling in the laminate. The effect of this unblocking requirement can be seen in Table 3, where increases in the number of plies do not necessarily bring improvements in running load capacity. In the worst case, the best 19 ply fully orthotropic laminate is outperformed in outright load carrying capacity by the best 17 ply laminate with respect to damage tolerance. Furthermore, the inclusion of progressively more 0º and 90º fibres in the thicker layups acts to reduce the full laminate Poisson's ratio, a property that in the past has been shown to help laminates resist localized delamination buckling[18]. Omitting the minimum ply percentage rule from the manufacturing constraints made these high Poisson's ratios possible, especially in the thinner laminates (7-14 plies thick). These designs did not include 90º fibres, the presence of which would reduce the Poisson's ratio significantly. Such designs could be less practical in a skin/stiffener configuration, as matching such high Poisson's ratios to other laminates might be troublesome.

For the design space investigated here, it has been shown that the inclusion of non-symmetric, fully uncoupled layups has not been of benefit with regards to damage tolerance. In all instances it is an anti-symmetric design that offers the best damage tolerance, and as such these solutions do not offer differing damage tolerances for each face. The gap between the best anti-symmetric and non-symmetric layup is generally small however, indicating that non-symmetric layups are not a great disadvantage in terms of damage tolerance. It is

interesting to note that with the constraint of full orthotropy applied, the most damage tolerant symmetric laminates are in all cases no better than either the best anti-symmetric or non-symmetric solution. When both full orthotropy and damage tolerance are required, symmetric laminates do not offer the best solution for laminates up to 21 plies thick.

The sensitivity of the best 21 ply laminate to errors in buckling strain prediction was explored by plotting buckling/threshold strain curves for each of the possible sublaminates, Fig. 4. For this laminate the critical interface is ply level 4. Figure 4 shows that the buckling strain for this interface lies near the turning point, and threshold strain is less sensitive to changes in buckling strain than for interfaces 1, 2 and 5. As with the 19 ply results shown in Fig. 3, at extremes of buckling strain the error ratio between buckling strain and threshold strain does not exceed 1. The majority of laminates investigated in this work tend to have their critical interface at the 25% boundary for thin film buckling behaviour. This means that those thin laminates tested here will have low values of buckling strain, i.e. sublaminate responses on the left of the 1 and 2 ply curves shown in Fig. 4. Thicker laminates will be critical for sublaminates 4 or 5 plies thick, with buckling occurring to the right of the point of minimum threshold strain on these curves. It is in these regions that the error transmitted from buckling strain estimation to threshold strain is largest, and this helps to explain the error data shown in Fig. 7.

As can be seen in Fig. 7, non-conservative errors in threshold strain are less than 1% for all layups. Average errors for each ply count are below 0.1%. These results are excellent when one accounts for the reduction in computation time achieved. Exhaustive analysis of all 69,140 fully orthotropic laminates up to 21 plies thick on a standard desktop PC takes in the order of 2 days to complete, with the implementation of parallel processing on a quad-core CPU. Analysis of the same design space using the surrogate, including all VICONOPT analyses required to build the model, takes approximately 18 minutes, around 0.625% of full

analysis. The surrogate model presented here has practical applications beyond the fully orthotropic case study provided. As a facilitator of an exhaustive search it allows users to find an optimum damage tolerant laminate from within any given design space without uncertainty over whether the solution is a true optimum, so often the case with typical optimisation techniques used in laminate optimisation, such as genetic algorithms. These design spaces may contain many millions of designs, but would still be manageable using the surrogate method.

10 Conclusion

CAI analysis of fully orthotropic laminates up to 21 plies thick has shown that the inclusion of non-symmetric laminates in the potential design space does not allow for higher threshold stresses than anti-symmetric layups. However, non-symmetric designs do not show a significant disadvantage from the point of view of damage tolerance, under the assumption that the laminate requires only one damage tolerant face, and are not outperformed by symmetric laminates at any ply count. For some laminate thicknesses it was found that adding plies may actually reduce overall load capacity as a result of ply unblocking and the requirement for full orthotropy. For laminates more than 14 plies thick, the maximum damage tolerant strength achieved was between 400 and 480 MPa. It was found that two types of damage tolerant laminate dominate, one without 90º plies and high Poisson's ratio, the other with one or two 90º plies and lower Poisson's ratio. The use of a simple surrogate sublaminate buckling model reduced computation time by over 99%, the results of which showed average errors less than 0.1%, and maximum non-conservative errors less than 1%.

11 References

[1]Rhead, A.T., and Butler, R., "Compressive Static Strength Model for Impact Damaged Laminates," *Composites Science and Technology*, Vol. 69, No. 14, 2009, pp. 2301-2307.

[2]Rhead, A.T., Butler, R., and Baker, N., "Analysis and Compression Testing of Laminates Optimised for Damage Tolerance," *Applied Composite Materials*, in press, DOI 10.1007/s10443-010-9153-z.

[3]Williams, F.W., Kennedy, D., Butler, R., and Anderson, M.S., "VICONOPT: Program for Exact Vibration and Buckling Analysis of Prismatic Plate Assemblies," *AIAA Journal*, Vol. 29, No. 11, 1991, pp. 1927-1928.

[4]Rhead, A.T., Butler, R., and Hunt, G.W., "Post-Buckled Propagation Model for Compressive Fatigue of Impact Damaged Laminates," *International Journal of Solids and Structures*, Vol. 45, No. 16, 2008, pp. 4349-4361.

[5]Thompson, J.M.T., and Hunt, G.W., *Elastic Instability Phenomena*, 1st ed., Wiley and Sons, London, 1984, pp. 171.

[6]Chai, H., Babcock, C.D., and Knauss, W.G., "One Dimensional Modelling of Failure in Laminated Plates by Delamination Buckling," *International Journal of Solids and Structures*, Vol. 17, No. 11, 1981, pp. 1069-1083.

[7]Rhead, A.T., and Butler, R., "Buckling, Propagation and Stability of Delaminated Anisotropic Layers," *14th European Conference on Composite Materials*, 684-ECCM14, Budapest, Hungary, 2010.

[8]Butler, R., Rhead, A.T., Liu, W., and Kontis, N., "Compressive Strength of Delaminated Aerospace Composites," *Philosophical Transactions of the Royal Society Part A* (submitted), 2011.

[9]Engineering Sciences Data Unit, "Laminate Stacking Sequences for Special Orthotropy (Application to Fibre Reinforced Composites)," ESDU Item No. 82013, 1982.

[10]Bartholomew, P., "Ply Stacking Sequences for Laminated Plates having In-Plane and Bending Orthotropy," *Fibre Science and Technology*, Vol. 10, No. 4, 1977, pp. 239-253.

[11]York, C.B., and Weaver, P.M., "Balanced and Symmetric Laminates – New Perspectives on an Old Design Rule," *51st AIAA/ASME/ASCE/AHS/ASC Structures, Structural Dynamics and Materials Conference*, AIAA-2010-2775, AIAA, Orlando FL, 2010.

[12]York, C.B., "Characterization of Nonsymmetric Forms of Fully Orthotropic Laminates," *Journal of Aircraft*, Vol. 46, No. 4, 2009, pp. 1114-1125.

[13]Hinton M. J., Kaddour A. S. and Soden P. D., "Failure Criteria in Fibre Reinforced Polymer Composites: The World-Wide Failure Exercise," Elsevier Science Ltd, 2004, Oxford, UK.

[14]Kaddour, A. S. and Hinton M. J., "Failure Criteria for Polymer Composites under 3D Stress States: The Second World-Wide Failure Exercise," Proc. *17th International Conference on Composite Materials*, Paper No. F12:1, 2009, Edinburgh, Scotland.

[15]Kaddour, A. S., Hinton M. J., Li, S. and Smith, P. A., "Damage Prediction in Polymer Composites: Update of Part A of the Third World-Wide Failure Exercise (WWFE-III)," *Proc. 17th International Conference on Composite Materials*, Paper No. F12:7, 2009, Edinburgh, Scotland.

[16]Liu, W., Butler, R., Mileham, A.R., and Green, A.J., "Bilevel Optimisation and Postbuckling of Highly Strained Composite Stiffened Panels," *AIAA Journal*, Vol. 44, No. 11, 2006, pp. 2562-2570.

[17]Niu, N.C.Y., *Composite Airframe Structures*, 2nd ed., Conmilit Press Ltd., Hong Kong, 1996, pp. 193.

[18]Baker, N., and Butler, R., "Compression after Impact Modeling of Damage Tolerant Composite Laminates," *51st AIAA/ASME/ASCE/AHS/ASC Structures, Structural Dynamics and Materials Conference*, AIAA-2010-2868, AIAA, Orlando FL, 2010.

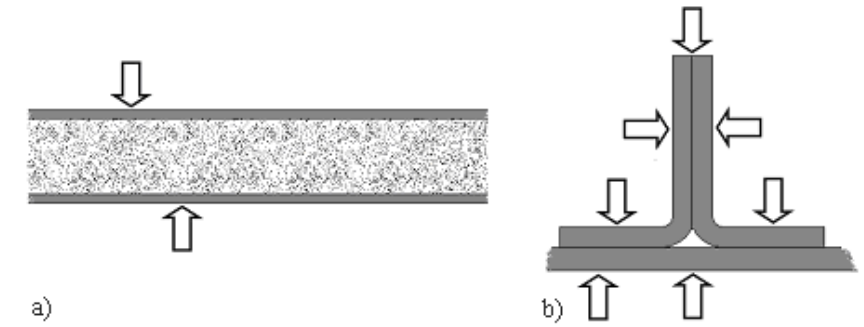

Figure 1. Cross-sections of composite features for which laminate non-symmetry may be desirable. (a) Sandwich panel face. (b) Stiffener flange. Arrows indicate directions of impact threats.

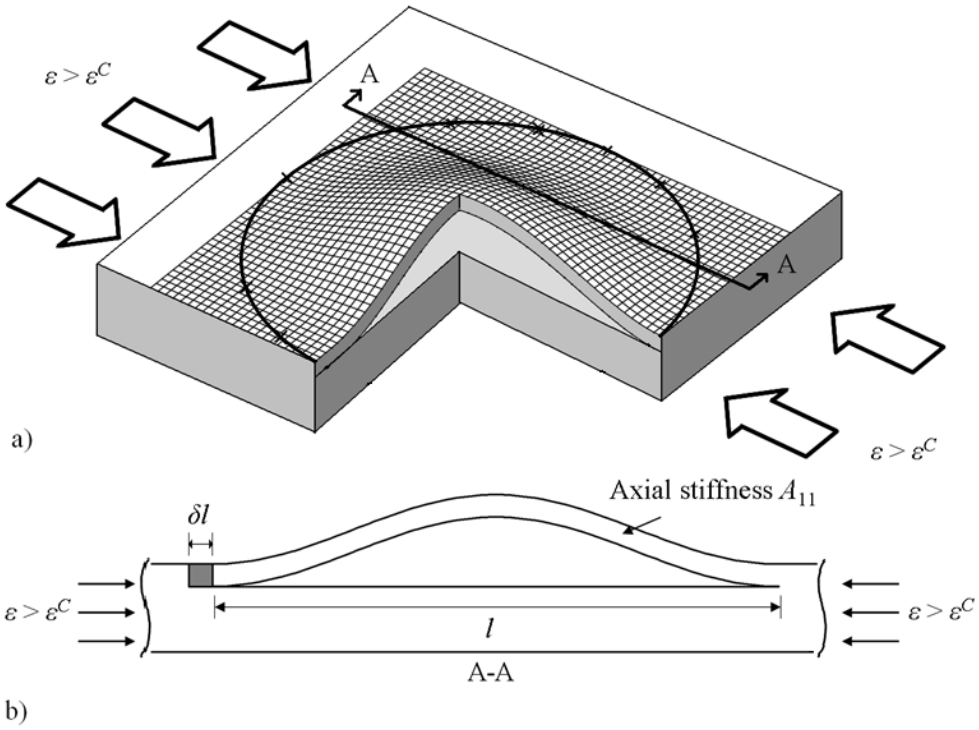

Figure 2. Cutaway of sublaminate buckling above delamination, showing a) the buckled thin film over a flat substrate, and b) section A-A displaying region δl into which the delamination propagates.

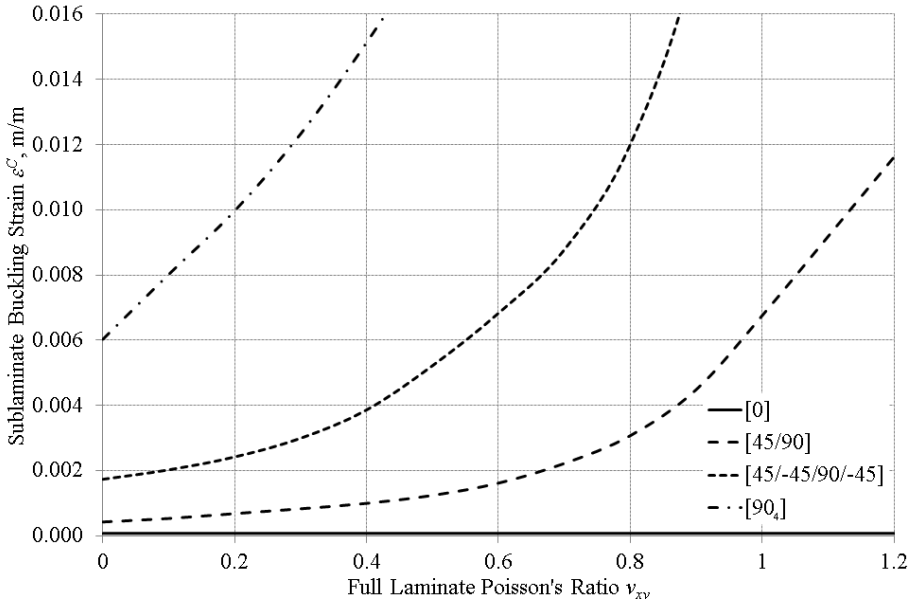

Figure 3. Relationship between full laminate Poisson's ratio and sublaminate buckling strain for selected sublaminates.

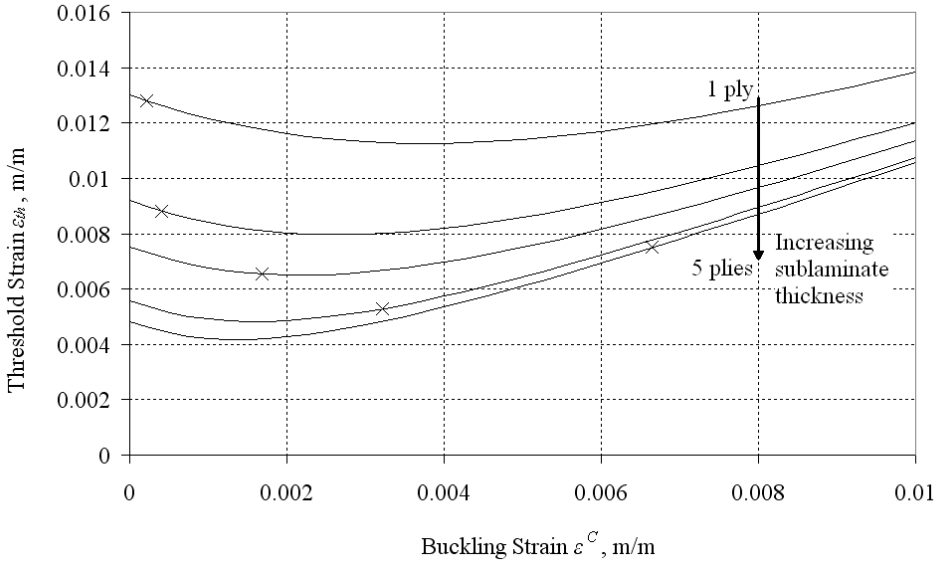

Figure 4. Relationship between buckling strain and threshold strain selected sublaminates in the 21 ply solution shown in Table 3.

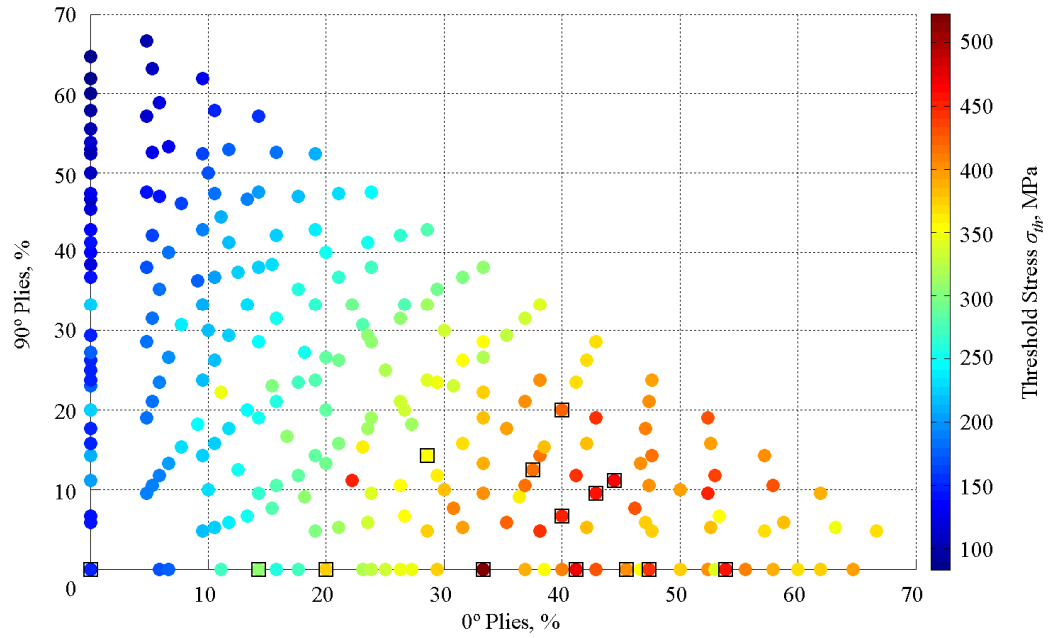

Figure 5. Threshold stress of fully orthotropic laminates by ply percentage breakdowns. Best designs for each ply count are boxed for clarity.

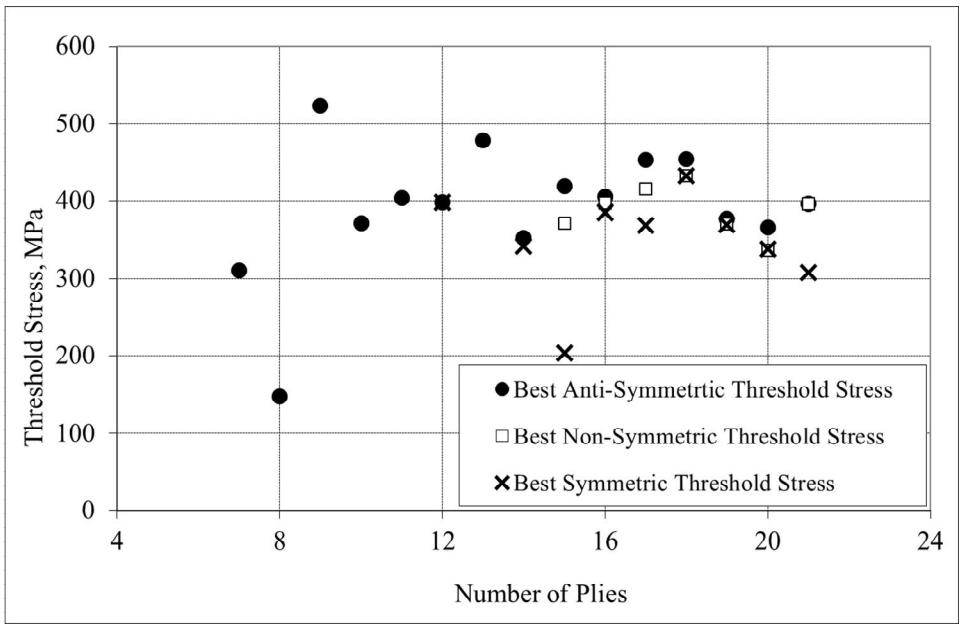

Figure 6. Threshold stress of fully orthotropic laminates by ply count.

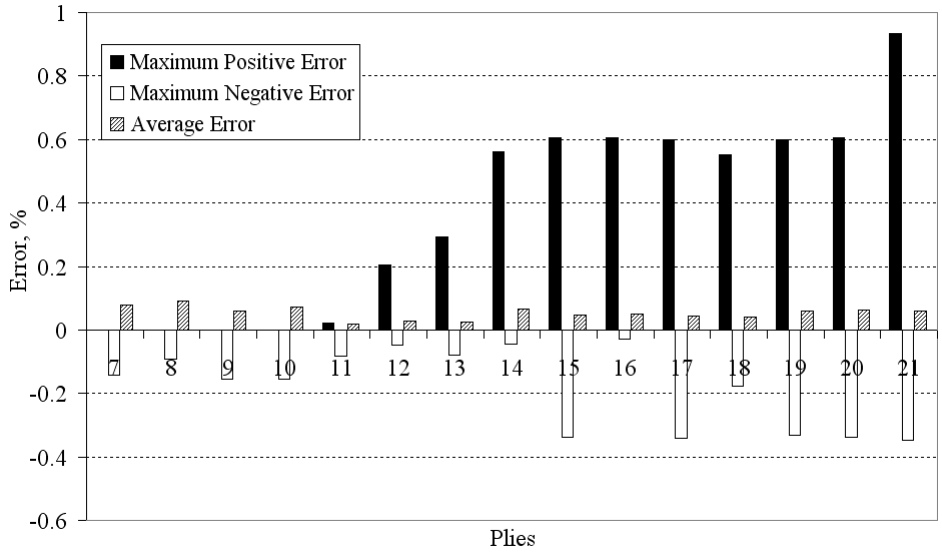

Figure 7. Error data for threshold strains calculated using linear interpolation of buckling strain data. Positive error is non-conservative.

	Number of plies, *n*														
	7	8	9	10	11	12	13	14	15	16	17	18	19	20	21
Symmetric	-	-	-	-	-	4	-	12	4	33	50	110	120	352	344
Anti-symmetric	2	1	6	6	24	21	84	76	288	268	1,002	934	3,512	3,290	12,392
Non-symmetric	-	-	-	-	-	-	-	-	68	59	780	559	4,934	4,284	35,521

Table 1. Number of symmetric, anti-symmetric and non-symmetric fully uncoupled laminates with 7 through 21 plies.

Material	E_{11} (GPa)	E_{22} (GPa)	G_{12} (GPa)	ν_{12}	t (mm)	G_{IC} (J/m^2)
HTA12K/977-2[16]	147	8.5	4.9	0.30	0.125	478

Table 2. Material Properties.

Plies	Layup	Threshold Stress σ_{th}, MPa	Running Load, kN/mm	Effective Modulus E_{xx}, GPa	Poisson's Ratio ν_{xy}
7	$[45/-45/-45/0/45/45/-45]_T$	308	0.27	36.3	0.769
8	$[45/-45/-45/45]_A$	148	0.15	17.8	0.783
9	$[45/-45/0/-45/0/45/0/45/-45]_T$	523	0.59	61.3	0.742
10	$[45/-45/-45/45/0]_A$	372	0.47	43.8	0.762
11	$[45/0/-45/-45/0_3/45/45/0/-45]_T$	403	0.55	77.1	0.718
12	$[45/-45/-45/0/45/0]_A$	398	0.60	61.3	0.741
13	$[45/0/-45/0/-45/0_3/45/0/45/0/-45]_T$	460	0.75	88.1	0.696
14	$[45/-45/-45/45/0/90/0]_A$	352	0.62	60.1	0.432
15	$[45/-45/-45/45/0_3/90/0_3/-45/45/45/-45]_T$	447	0.84	73.0	0.538
16	$[45/-45/-45/45/0_2/90/0]_A$	415	0.83	71.0	0.429
17	$[45/-45/45/-45/0_2/-45/0_3/45/0_2/45/-45/45/-45]_T$	472	1.00	71.5	0.727
18	$[45/-45/-45/45/0_3/90/0]_A$	464	1.04	79.4	0.426
19	$[45/-45/45/-45/0_3/-45/0_3/45/0_3/45/-45/45/-45]_T$	440	0.90	79.6	0.713
20	$[45/-45/-45/45/90/0_3/90/0]_A$	423	1.06	74.1	0.308
21	$[45/-45/45/-45/90/0_3/-45/0_3/45/0_3/90/45/-45/45/-45]_T$	458	1.20	77.2	0.464

Table 3. Fully orthotropic laminates up to 21 plies thickness with highest CAI threshold stress, using VICONOPT buckling analysis. The subscript A denotes that the layup has symmetric crossplies, and anti-symmetric angle plies. Running load is the compressive load per unit width equivalent to σ_{th}.